Optical Engineering

SPIEDigitalLibrary.org/oe

Quadratic spatial solitons generated in periodically poled lithium tantalite

Wenjun Liu
Gang Yang
Xiang Lin
Lihui Pang
Shengli Fan

SPIE

Quadratic spatial solitons generated in periodically poled lithium tantalite

Wenjun Liu
Gang Yang
Xiang Lin
Lihui Pang
Shengli Fan
Harbin Institute of Technology at Weihai
Department of Optoelectronics Science
Weihai 264209, China
E-mail: liuwenjun68@siom.ac.cn

Abstract. The properties of quadratic spatial solitons generated in periodically poled lithium tantalite in the femtosecond regime are investigated. By using only a fundamental frequency beam as the input to excite quadratic spatial solitons, single and spatially anisotropic multiple solitons are generated. Our experiments demonstrate that the number of solitons is dependent on the input power. In the experiment, beam narrowing occurs first, leading to single-soliton generation. The threshold for multiple solitons is around 1.5 mW. The number of solitons does not increase indefinitely with input power. Multiple soliton generation only occurs in the input power range of 1.5 to 6.3 mW. The number of solitons decreases to 1 when the input power is 6.3 mW. The temporal and spectral characteristics of the spatial solitons are measured by using the GRENOUILLE technique. [DOI: 10.1117/1.OE.52.8.087103]

Subject terms: nonlinear optics; spatial solitons; lithium tantalite; periodically poled.

Paper 130606 received Apr. 18, 2013; revised manuscript received Jun. 13, 2013; accepted for publication Jun. 28, 2013; published online Aug. 1, 2013.

1 Introduction

With the development of high power ultrafast lasers, quadratic nonlinear crystals have become widely used in nonlinear optics, and the quadratic spatial soliton is one of the most intriguing nonlinear effects.[1–10] One of the unique features of quadratic solitons is that they consist of all of the beams strongly coupled together by the second-order nonlinearity. Second-harmonic generation (SHG) processes can result in generation of quadratic spatial soliton. With their particle-like behavior in interactions and collisions, spatial solitons have the potential to be used for all-optical data processing, pattern recognition, and parallel information storage.[11–13]

The quadratic spatial soliton is different from other types of spatial solitons. First, the quadratic spatial soliton relies solely on second-order nonlinearities. Second, the optical field does not modify any property of the medium. Third, the self-trapped soliton exists by virtue of the strong interaction and energy exchange between two or more beams with different frequencies. In SHG, this means at least one fundamental field and at least one harmonic field. The fundamental field and the second harmonic (SH) affect each other via upconversion and downconversion processes when the solitons overlap. The total electromagnetic energy is conserved. In SHG, it is common for the energy propagation directions of the fundamental and harmonic beams to be different. As long as the walk-off distance is less than the gain length, the fundamental and harmonic beams are locked in space and copropagate together as quadratic spatial solitons.

The quasi-phase matching (QPM) technique is becoming increasingly popular. QPM offers a large nonlinearity and phase-matching capability at convenient wavelengths. Ferroelectric nonlinear crystal materials which are suitable for periodic poling include lithium niobate ($LiNbO_3$), lithium tantalate ($LiTaO_3$), potassium titanyl phosphate ($KTiOPO_4$), and potassium titanyl arsenate ($KTiOAsO_4$). These nonlinear crystals are often used in optical parametric oscillators and frequency doublers, and they are also available in the form of nonlinear waveguides. Quadratic spatial solitons generated in periodically poled $LiNbO_3$, $KTiOPO_4$, and $KTiOAsO_4$ in the picosecond regime have been investigated.[14–20] In this article, quadratic spatial solitons generated in periodically poled lithium tantalite (PPLT) in the femtosecond regime are investigated. By using only a fundamental frequency beam as an input, we are able to observe a single soliton and spatially anisotropic multiple solitons. The temporal and spectral characteristics of the quadratic spatial solitons are measured by using grating-eliminated no-nonsense observation of ultrafast incident laser light e-fields (GRENOUILLE) technique.[21,22]

2 Theory

Quadratic spatial solitons consist of beams which are strongly coupled by second-order nonlinearities under the conditions of wave-vector conservation. Here, we consider a nonlinear optical system with two beams. One beam is the fundamental wave (FW) and the other is the generated SH wave. The evolution of the electric fields with propagation along z is given by the coupled equations:

$$\frac{\partial}{\partial z}E_{\mathrm{FW}} - i\frac{1}{2k_{\mathrm{FW}}}\left(\frac{\partial^2}{\partial x^2}+\frac{\partial^2}{\partial y^2}\right)E_{\mathrm{FW}} = i\frac{\omega^2 d_{\mathrm{eff}}}{k_{\mathrm{FW}}c^2}E_{\mathrm{SH}}E_{\mathrm{FW}}^{*}\exp(-i\Delta k z) \quad (1)$$

and

$$\frac{\partial}{\partial z}E_{\mathrm{SH}} - i\frac{1}{4k_{\mathrm{FW}}}\left(\frac{\partial^2}{\partial x^2}+\frac{\partial^2}{\partial y^2}\right)E_{\mathrm{SH}} = i\frac{\omega^2 d_{\mathrm{eff}}}{k_{\mathrm{FW}}c^2}E_{\mathrm{FW}}^{2}\exp(i\Delta k z), \quad (2)$$

where E_{FW} and E_{SH} are the complex amplitude of the FW and SH waves, respectively. $\Delta k = 2k_{FW} - k_{SH}$ is the phase mismatch. k_{FW} is the wave numbers of the FW and k_{SH} is that of the SH wave. Δk depends on the wavelength, material temperature, and polarization of the propagating beam. The first equation describes downconversion, and the second one describes upconversion. The terms on the left-hand sides of the equations describe the change of the complex amplitude of the FW and the SH wave due to diffraction. The terms on the right-hand sides are the source terms. The generation of the SH is driven by the term E_{FW}^2. The generated SH is initially narrower than the fundamental beam. The fundamental beam is regenerated via the product $E_{FW}^* E_{SH}$, and if the SH field is narrower than the fundamental beam, this regenerated field is also narrower than the part of the fundamental field that has not been converted to the SH harmonic. Therefore, both the beams undergo a mutual focusing effect due to energy exchange. If this occurs over a distance comparable to the diffraction length, the mutual focusing effect can result in mutually locked solitons. In general, the nonlinear solutions consist of a combination of fundamental and harmonic fields. However, these solutions are not stable and any noise perturbations will cause both beams to break up into multiple spatial solitons.

3 Experiments

The experimental setup is shown in Fig. 1. A Ti:sapphire regenerative amplified laser system generates 120-fs pulses with a central wavelength of $\lambda = 800$ nm, and the pulses' repetition rate is 1 kHz. To achieve a high degree of coherence, a spatial filter is applied. The laser power is controlled by an attenuator. The laser is polarized parallel to the c axis of the PPLT in order to use its largest quadratic nonlinear coefficient d_{33}. The beam is focused onto the entrance surface of the PPLT sample by a converging lens with a focal length of $f = 10$ cm. The spot diameter of the focused beam is 25 μm, which is equivalent to about three diffraction lengths along the propagation axis. The PPLT is fabricated by using the electric-field-poling technique. The poling period is 8.64 μm. The PPLT crystal is 15 mm long and 0.5 mm thick, and it is mounted on a temperature-controlled oven. In the experiment, a magnified image of the output beam at the exit surface of the PPLT crystal is recorded by a charge-coupled device (CCD) camera connected to a beam analyzer. Two different filters are alternately introduced to select either the FW or the SH beam.

4 Results and Discussion

In the experiment, for a sufficiently high fundamental input power, energy is quickly converted to the SH wavelength, and the two fields then evolve toward a quasi-steady state.

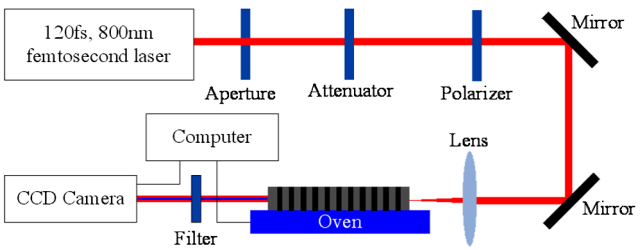

Fig. 1 Schematic of experimental setup.

This quasi-steady state is accompanied by reshaping and self-trapping of waves and corresponds to the birth of a quadratic spatial soliton.

The SH power efficiency as a function of crystal temperature is shown in Fig. 2. Crystal temperature is controlled by an oven with a temperature stability of 0.10°C. The input FW power is on the order of several milliwatts in order to satisfy the low-depletion-limit condition. The phase-matching temperature is 224°C. The full width at half maximum bandwidth temperature is about $\Delta T = 60$°C, which is highly advantageous for maintaining the energy stability of the soliton. The experiments are performed at a temperature of 200°C, corresponding to a phase mismatch of $\sim 43\pi$ for z axis propagation.

A typical method for verifying soliton formation is to compare the input and the output beam sizes. For our experience, the measured dependence of the output FW beam size on input intensity is shown in Fig. 3. The solid circles and the line in Fig. 3 are the measured data and the fitted curve, respectively. The FW becomes self-trapped when the input power is 0.4 mW. Two solitons appear when the input power is 1.5 mW. At a sufficiently high fundamental input power, extra multiple solitons appear.

Figure 4 shows the experimental results for single-soliton generation for three different input powers. The calculated

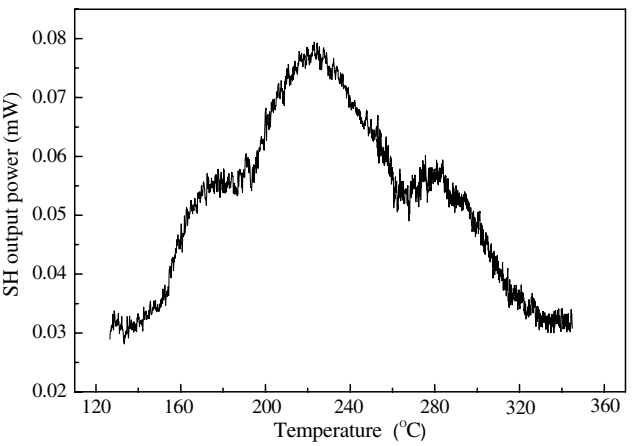

Fig. 2 Second harmonic (SH) power as a function of the sample temperature.

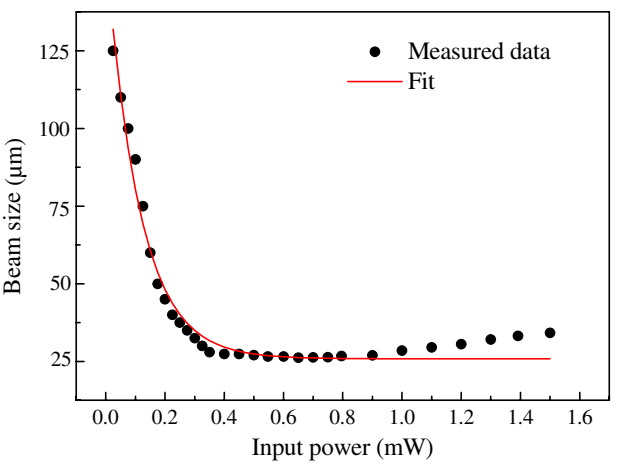

Fig. 3 Dependence of the output fundamental wave (FW) beam size on the input intensity.

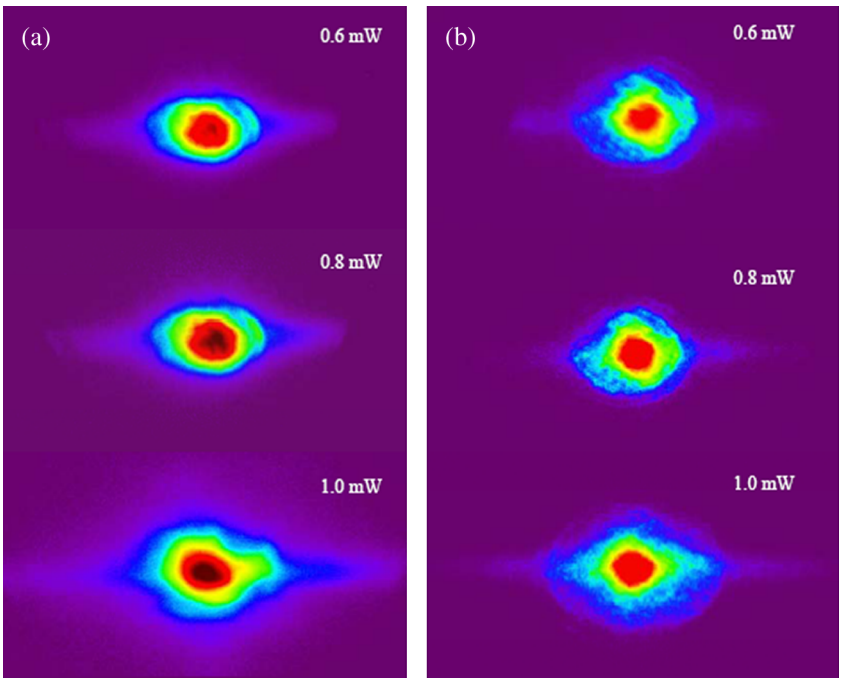

Fig. 4 Single-soliton generation: (a) fundamental and (b) SH output patterns.

evolution of the fundamental and harmonic beams for different input powers is shown in Fig. 5. A circular input beam is assumed in the calculation. The radiation cones appear approximately as circles with specific radii centered on the beam axis. In the process of soliton formation, the excitation conditions might be very far from the stationary soliton solutions, and large amounts of radiation might be emitted. Additional solitons can be generated from the radiation.[4,9,11,21] Increasing the input power leads to multisoliton generation. The output multiple-soliton patterns can be random due to spatial or temporal noise introduced by the incident femtosecond pulsed beam. The multiple-soliton patterns of the SH wave pumped with different input powers are demonstrated in Fig. 6. Multiple-soliton generation can be clearly

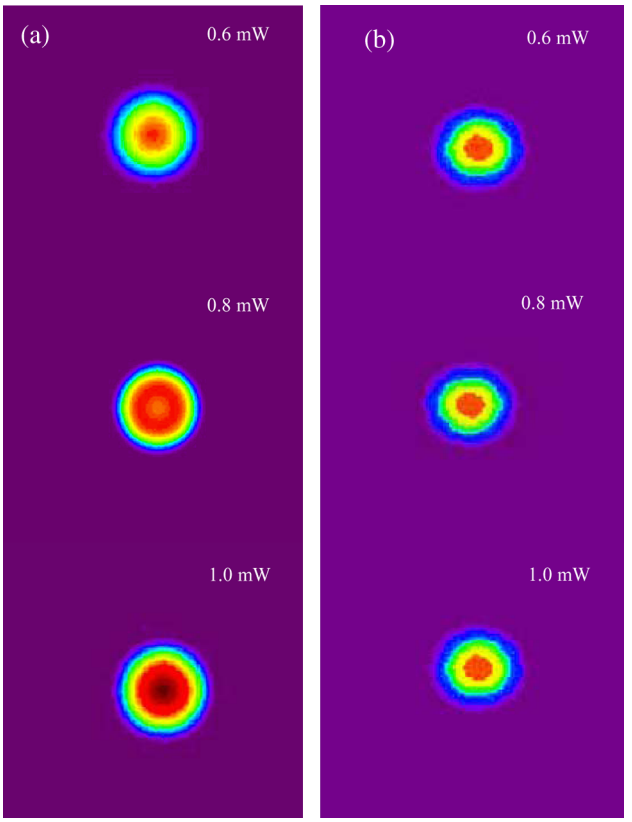

Fig. 5 Calculated evolution of (a) the fundamental beam and (b) harmonic beam for different input powers.

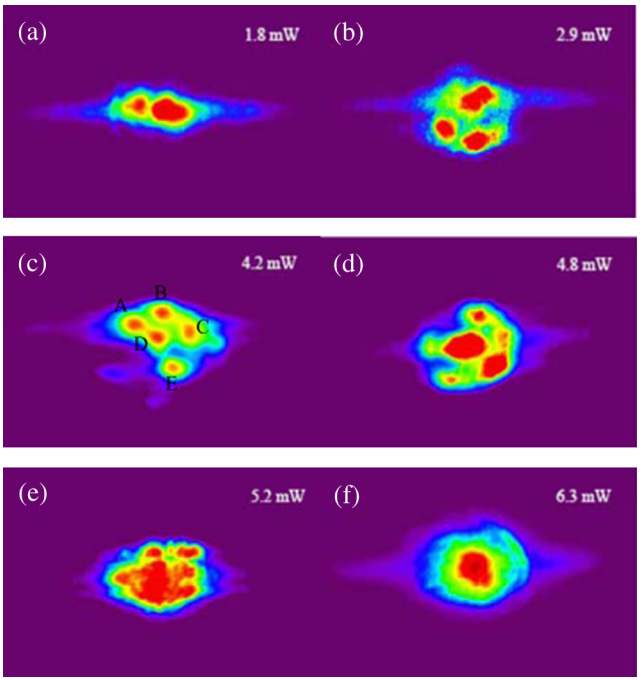

Fig. 6 SH multiple-soliton generation output patterns pumped with different input powers. (a) 1.8 mW, (b) 2.9 mW, (c) 4.2 mW, (d) 4.8 mW, (e) 5.2 mW, and (f) 6.3 mW.

seen, and the output patterns consist of irregularly shaped beams, where several beams exist at the same time with the potential to interact and merge. What happens at the FW in the region of 1.8 to 4.8 mW is similar to that of what the SH does, and not provided here for brevity.

There is an evidence for multisoliton generation at input powers of about 1.5 mW and higher. In Fig. 6(a), the predominant pattern consists of two localized beams aligned horizontally. Two well-defined and separated soliton spots appear. At higher input power, three and five solitons are generated as shown in Fig. 6(b) and 6(c). Much more complex and chaotic output patterns appeared with a further increase in the input power as shown in Fig. 6(d) and 6(e), and the soliton-like spots were no longer nicely shaped. With further increasing input power, the number of solitons decreases to 1 as shown in Fig. 6(f). Here, additional solitons are prohibited from escaping from the propagation axis, resulting in single-soliton generation again. The different

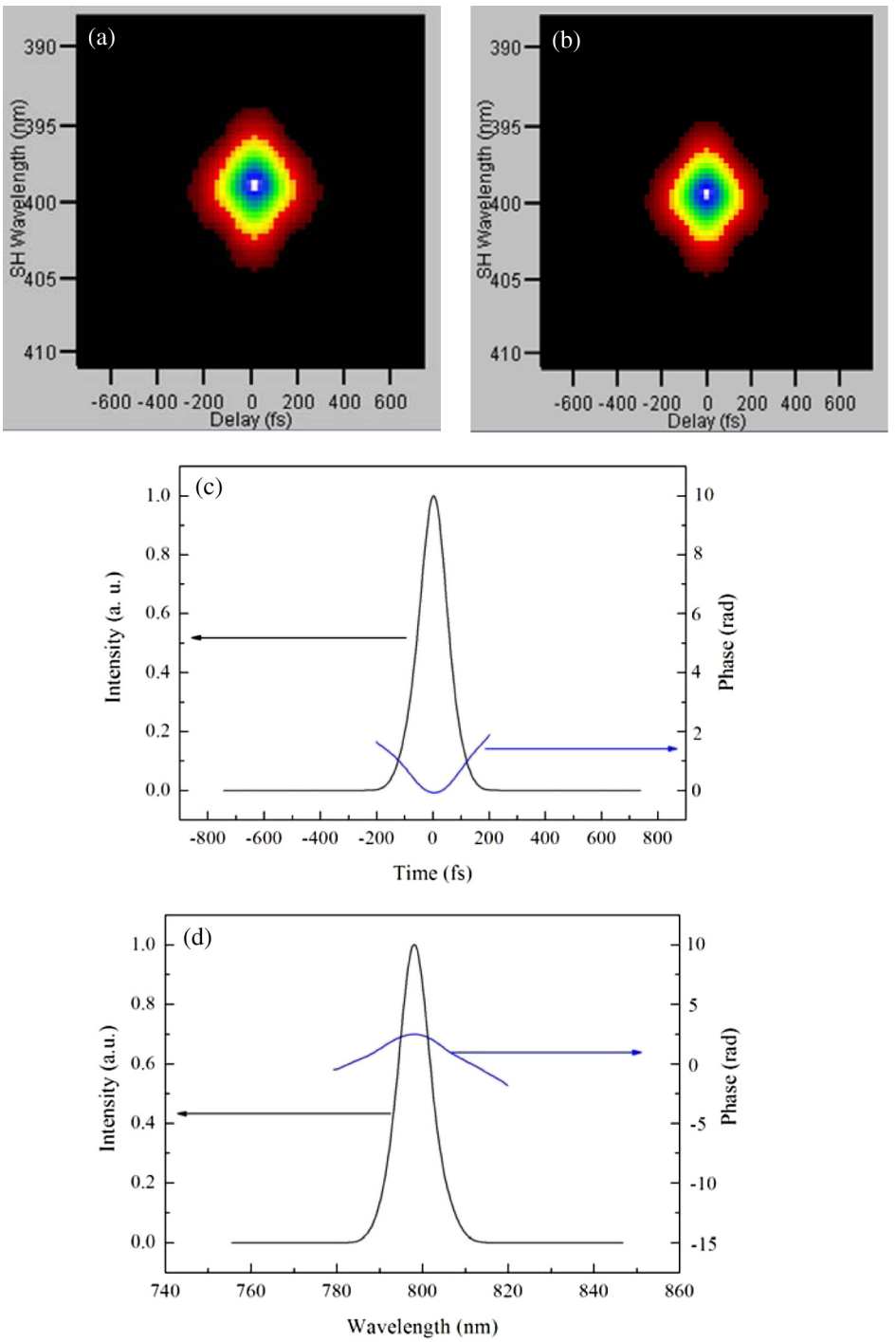

Fig. 7 (a) Measured trace, (b) retrieved trace, (c) temporal profile and temporal phase, and (d) spectrum and spectral phase of a FW spatial soliton with a pump power of 0.8 mW.

patterns in Fig. 6 are driven by the inherent spatiotemporal dynamics generated in the upconversion and downconversion processes, and a small amount of spatiotemporal noise can lead to multiple solitons into random patterns.[21–24]

All the images exhibit irregular shapes and the different spots carry different energies. Multiple solitons were observed near phase matching, which might attribute to anisotropic diffraction in crystal and asymmetries in the input beam. For near the phase-matching condition in a biaxial crystal, the SH Poynting vector is not parallel to that of the FW. Because the energy exchange between the FW and SH depends on their overlap in space, this leads to a distortion of both beams along the walk-off direction. The refractive index surfaces for the FW and SH touch each other for propagation along a crystal axis. However, the local radii of curvature of the surfaces are spatially anisotropic. As a result, both the diffraction and the phase mismatch are spatially anisotropic and increase differently with angular

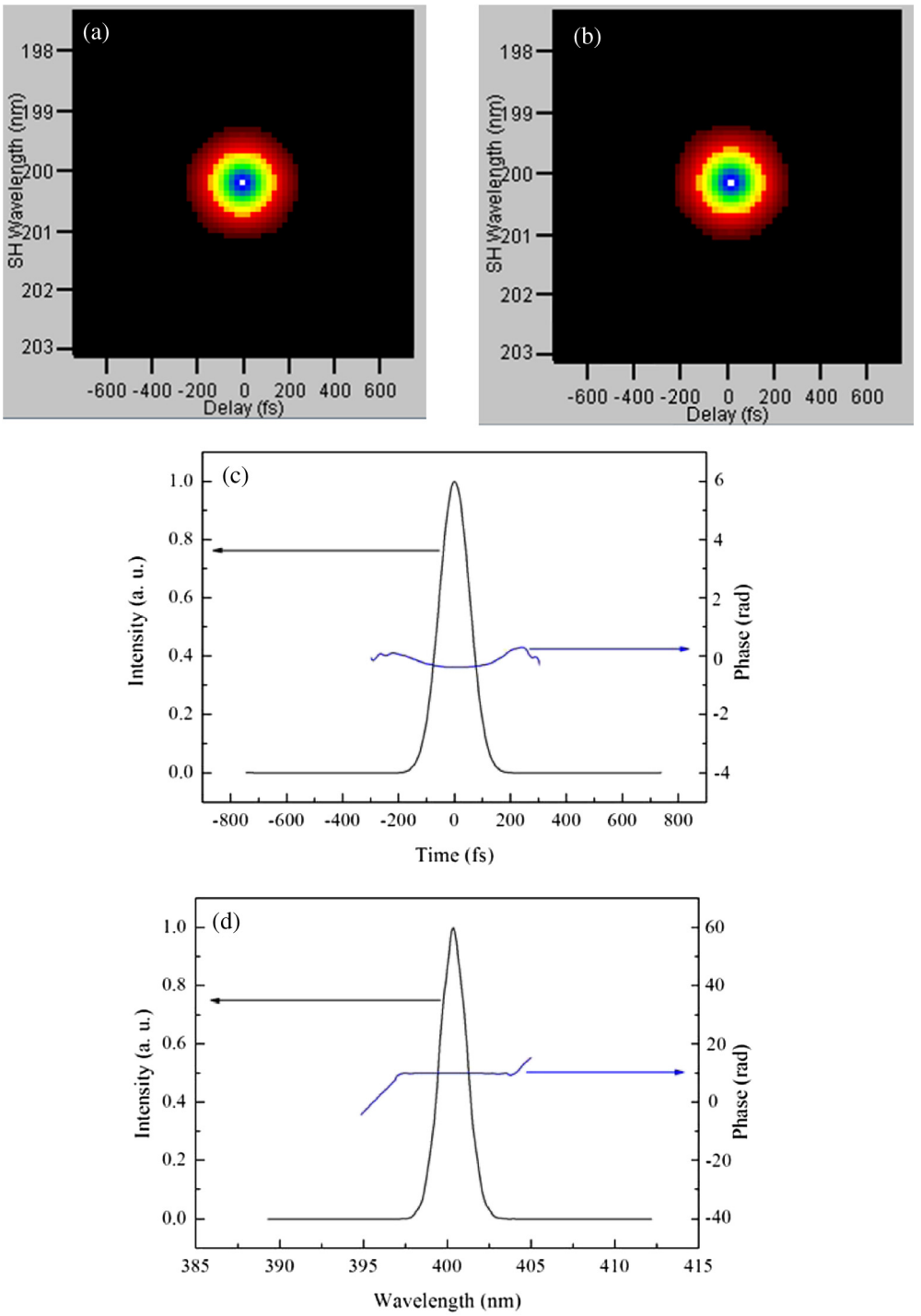

Fig. 8 (a) Measured trace, (b) retrieved trace, (c) temporal profile and temporal phase, and (d) spectrum and spectral phase of a SH spatial soliton with a pump power of 0.8 mW.

detuning from the two crystal axes. This anisotropy determines the direction into which spatial solitons are generated for incident fundamental beams that carry sufficient energy to generate multiple solitons. If only anisotropic diffraction in crystal is presented, the images of shapes should be symmetrical. However, beam asymmetries and noise contribute to the variations in the positions and spatial orientation of the multiple solitons. It has been shown that there is one mechanism which breaks the cylindrical symmetry of the radiation fields and can lead to multiple solitons forming out of the radiation cones,[10,25] which occurs when an asymmetric beam is incident, leading to spatially anisotropic up- and downconversion processes and hence to multiple solitons being generated. When both the anisotropic diffraction in crystal and asymmetries in the input beam are present, the anisotropic diffraction of PPLT and beam shape contributions can either interfere constructively or destructively, depending on the detailed circumstances.[25] The excitation is pulsed laser, and different parts of the pulse will undergo different dynamical routes. It can also affect other properties of multisoliton generation.[10]

The dependence of the number of solitons is demonstrated experimentally to have complex input intensity dependence. It does not increase indefinitely with intensity, but multisoliton generation only occurs in a range of input powers. The threshold for multisoliton generation depends on the magnitude of the beam ellipticity.[10] For a given crystal length, there is a well-defined threshold for the onset and disappearance of multisoliton generation. Inphase solitons are formed near the incident beam axis and they experience attractive forces and energy exchange with both the central soliton and each other due to their small initial separation. They are also formed with the transverse momentum associated with the diverging radiation. Thus, their subsequent

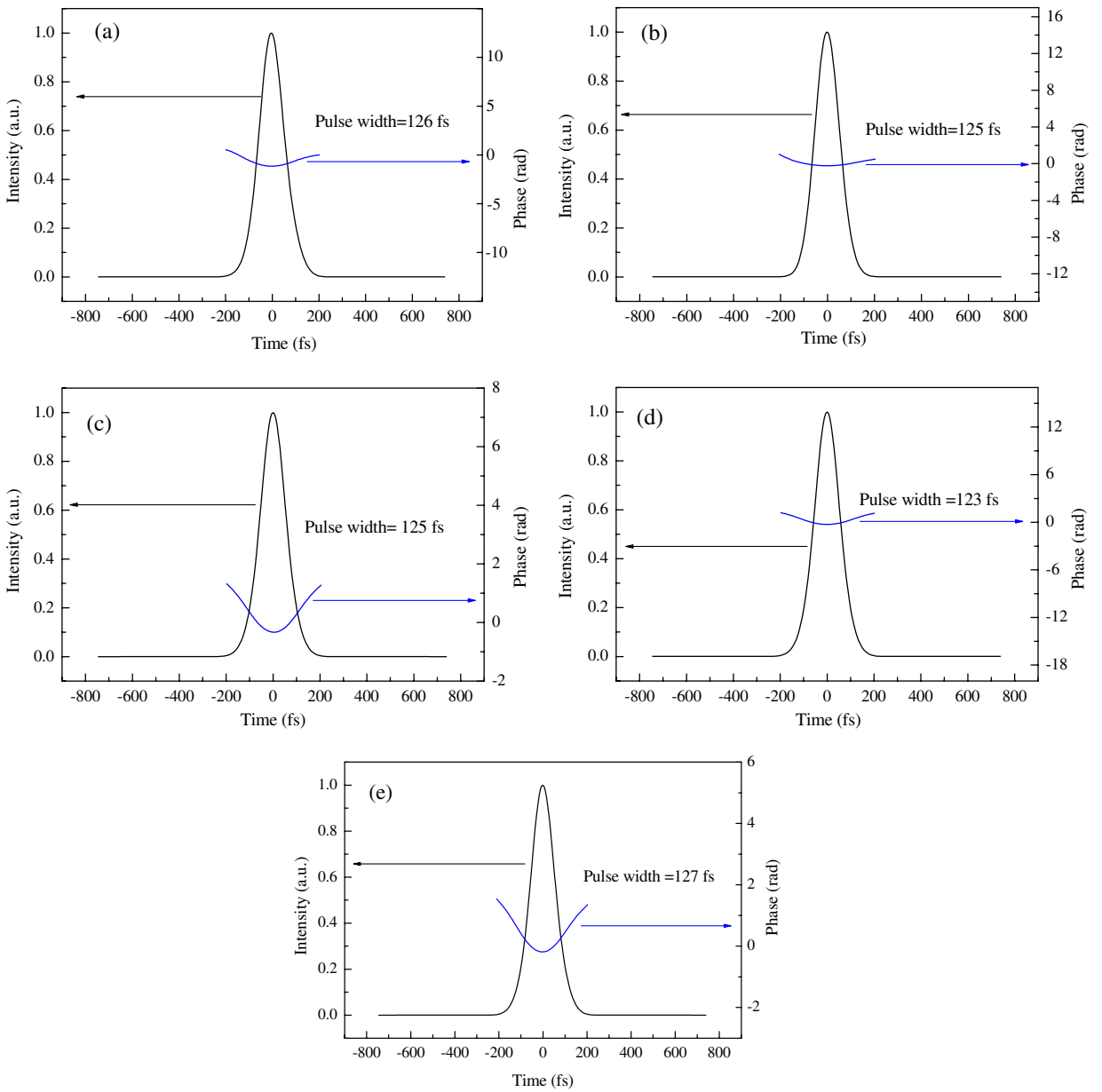

Fig. 9 Temporal profile and temporal phase of multiple SH spatial soliton with a pump power of 4.2 mW as shown in Fig. 6(c). (a) A-pulse width 126 fs, (b) B-pulse width 125 fs, (c) C-pulse width 125 fs, (d) D-pulse width 123 fs, (e) E-pulse width 127 fs.

dynamics involves a trade-off between this initial transverse momentum and the attractive forces. As a result, it is even possible for the central soliton to be eliminated completely and all of the self-trapped energy to appear in the satellite solitons. As the input intensity increases, the attractive forces become stronger and the divergence becomes weaker. For large enough incident intensities, the attractive forces are strong enough to force all of the localized beams to collapse back to the center soliton.[25]

In the experiment, the temporal and spectral characteristics of the spatial solitons are also measured by using the GRENOUILLE technique. Figure 7 shows the results for a fundamental soliton with a pump power of 0.8 mW. Figure 7(a) and 7(b) shows the measured and retrieved traces, respectively. The temporal profile and phase are illustrated in Fig. 7(c), and the pulse width is 121 fs. This indicates that the temporal pulse compression and quasi-spatiotemporal solitons cannot be generated in uniform PPLT. The pulse compression and shaping can be obtained only by nonuniform or chirped quasi-phase-matching gratings.[26–28] Figure 7(d) shows the spectrum and spectral phase, the spectrum is centered at 800 nm, and the spectral width is 8.7 nm.

The temporal and spectral characteristics of an SH spatial soliton generated with a pump power of 0.8 mW are shown in Fig. 8. Figure 8(a) and 8(b) shows the measured and retrieved traces, respectively. The temporal profile and phase are illustrated in Fig. 8(c) and the pulse width is 125 fs. Figure 8(d) shows the spectrum and spectral phase, where the spectrum is centered at 400 nm and the spectral width is 2 nm.

Figure 9 shows the temporal profile and phase of each of the solitons in Fig. 6(c) labeled a, b, c, d, and e. The temporal widths of the multiple spatial solitons are 126, 125, 125, 123 and 127 fs, respectively; these temporal widths are in better agreement with that of a single soliton. The minor difference of temporal widths of multiple solitons might attribute to random error. The traces and spectrum are abbreviated for clarity. The spectra of the multiple soliton are all centered at 400 nm, and the spectral widths are all centered at 2 nm.

5 Conclusions

The generation of single and multiple quadratic spatial solitons in PPLT in the femtosecond regime is investigated. It has been shown that the generation of multiple quadratic solitons in PPLT is a complex process, which is a consequence of using a fundamental beam only at the input. The additional solitons are formed by the off-axis, anisotropic solitons. This leads to a complex behavior involving a minimum intensity threshold for multisoliton generation and an upper threshold after which only single solitons are obtained. In this experiment, beam narrowing occurs first, leading to single-soliton generation. The threshold for multiple-soliton generation is around 1.5 mW. Two well-separated solitons are generated when the input power is 1.8 mW. Three solitons appear around an input power of 2.9 mW. Five solitons are formed around an input power of 4.2 mW. The number of multiple solitons does not increase indefinitely with input power. As the input power continues to increase, it is observed at an input power of 6.3 mW that the number of solitons decreases to 1. The temporal and spectral characteristics of the spatial solitons are also presented.

Acknowledgments

This work is supported by the National Natural Science Foundation of China (Grant No. 61178025).

References

1. W. E. Torruellas et al., "Observation of two-dimensional spatial solitary waves in a quadratic medium," *Phys. Rev. Lett.* **74**(25), 5036–5039 (1995).
2. R. Schiek, Y. Baek, and G. I. Stegeman, "One-dimensional spatial solitary waves due to cascaded second-order nonlinearities in planar waveguides," *Phys. Rev. E* **53**(1), 1138–1141 (1996).
3. S. Carrasco et al., "Quadratic solitons: existence versus excitation," *IEEE J. Sel. Top. Quantum Electron.* **8**(3), 497–505 (2002).
4. G. Assanto and G. Stegeman, "The simple physics of quadratic spatial solitons," *Opt. Express* **10**(9), 388–396 (2002).
5. C. Conti, M. Peccianti, and G. Assanto, "Observation of optical spatial solitons in a highly nonlocal medium," *Phys. Rev. Lett.* **92**(11), 113902-1–113902-4 (2004).
6. M. Pesch et al., "Two-dimensional front dynamics and spatial solitons in a nonlinear optical system," *Phys. Rev. Lett.* **99**(15), 153902-1–153902-4 (2007).
7. M. Petrović et al., "Two dimensional counter propagating spatial solitons in photorefractive crystals," *Phys. Rev. Lett.* **95**(05), 053901 (2005).
8. R. M. Wang et al., "Observation of multi-component spatial vector solitons of four-wave mixing," *Opt. Express* **20**(13), 14168–14182 (2012).
9. S. V. Polyakov and G. I. Stegeman, "Quadratic solitons in anisotropic media: variational approach," *Phys. Rev. E* **66**(4), 046622-1–046622-7 (2002).
10. S. Carrasco et al., "Observation of multiple soliton generation mediated by amplification of asymmetries," *Phys. Rev. E* **67**(4), 046616-1–046616-4 (2003).
11. L. Torner and G. I. Stegeman, "Multicolor solitons," *Opt. Photon. News*, **12**(6), 36–39 (2001).
12. A. V. Buryak et al., "Optical solitons due to quadratic nonlinearities: from basic physics to futuristic applications," *Phys. Rep.* **370**(2), 63–235 (2002).
13. Yu. S. Kivshar and G. P. Agrawal, "Optical solitons: from fibers to photonic crystals," Academic Press, New York (2003).
14. C. Y. Gao et al., "Shifting bright spatial solitons in LiNbO3," *Opt. Lett.* **37**(17), 3702–3704 (2012).
15. S. Polyakov et al., "Properties of quadratic multi-soliton generation near phase-match in periodically poled potassium titanyl phosphate," *Opt. Express*, **11**(11), 1328–1337 (2003).
16. W. K. Lee and T. S. Chan, "Experimental investigation of phase-dependent interactions of photovoltaic bright spatial solitons in photorefractive Fe:LiNbO3," *J. Opt. Soc. Am. B* **23**(9), 1920–1924 (2006).
17. P. Zhang et al., "One-dimensional spatial dark soliton-induced channel waveguides in lithium niobate crystal," *Appl. Opt.* **45**(10), 2273–2278 (2006).
18. B. Bourliaguet et al., "Observation of quadratic spatial solitons in periodically poled lithium niobate," *Opt. Lett.* **24**(20), 1410–1412 (1999).
19. H. Kim et al., "Quadratic spatial solitons in periodically poled KTiOPO4," *Opt. Lett.* **28**(8), 640–642 (2003).
20. H. Cui, B. Z. Zhang, and W. L. She, "Self-deflection suppression of bright spatial solitons in periodically poled photovoltaic photorefractive crystals," *J. Opt. Soc. Am. B* **25**(10), 1756–1762 (2008).
21. P. O'Shea et al., "Highly simplified device for ultrashort-pulse measurement," *Opt. Lett.* **26**(12), 932–934 (2001).
22. R. Trebino et al., "Simple devices for measuring complex ultrashort pulses," *Laser Photon. Rev.* **3**(3), 314–342 (2009).
23. R. Malendevich et al., "Two-dimensional type I quadratic spatial solitons in KNbO3 near non-critical phase-matching," *Opt. Lett.* **27**(8), 631–633 (2002).
24. L. Jankovic et al., "Interactions of quadratic spatial solitons in noncritically phase-matched KNbO3," *Laser Phys.* **14**(2), 264–272 (2004).
25. S. Polyakov et al., "Effects of anisotropic diffraction on quadratic multi soliton excitation in non-critically phase-matched crystals," *Opt. Lett.* **27**(12), 1049–1051 (2002).
26. M. A. Arbore et al., "Engineerable compression of ultrashort pulses by use of second-harmonic generation in chirped-period-poled lithium niobate," *Opt. Lett.* **22**(17), 1341–1343 (1997).
27. P. Loza-Alvarez et al., "Simultaneous femtosecond-pulse compression and second-harmonic generation in aperiodically poled KTiOPO4," *Opt. Lett.* **24**(15), 1071–1073 (1999).
28. G. Imeshev et al., "Ultrashort-pulse second-harmonic generation with longitudinally nonuniform quasi-phase-matching gratings: pulse compression and shaping," *J. Opt. Soc. Am. B* **17**(2), 304–318 (2000).

Wenjun Liu received his BE and MS from Shandong Normal University, and his PhD degree from Shanghai Institute of Optics and Fine Mechanics, Chinese Academy of Sciences. Currently, he is working as a research fellow at the Department of Optoelectronics Science, Harbin Institute of Technology at Weihai. His areas of interest are ultrafast measurement and nonlinear optics.

Gang Yang is studying for his MS at Harbin Institute of Technology at Weihai. His area of interest is nonlinear fiber optics.

Xiang Lin received his BE from Liaocheng University, and his MS from Harbin Institute of Technology at Weihai. Currently, he is studying for his PhD student at Harbin Institute of Technology. His areas of interest are nonlinear optics and laser spectroscopy.

Lihui Pang is studying for her MS at Harbin Institute of Technology at Weihai. Her area of interest is nonlinear fiber optics.

Shengli Fan is an undergraduate student at Harbin Institute of Technology at Weihai. His areas of interest are nonlinear fiber optics and photonic crystal fiber.